0026-895X/01/6001-164–173$3.00
MOLECULAR PHARMACOLOGY
Copyright © 2001 The American Society for Pharmacology and Experimental Therapeutics
Mol Pharmacol 60:164–173, 2001

Vol. 60, No. 1
766/911441
Printed in U.S.A.

Mutation of Asp^{171} and Asp^{262} of the Chemokine Receptor CXCR4 Impairs Its Coreceptor Function for Human Immunodeficiency Virus-1 Entry and Abrogates the Antagonistic Activity of AMD3100

SIGRID HATSE, KATRIEN PRINCEN, LARS-OLE GERLACH, GARY BRIDGER, GEOFFREY HENSON, ERIK DE CLERCQ, THUE W. SCHWARTZ, and DOMINIQUE SCHOLS

Rega Institute for Medical Research, Katholieke Universiteit Leuven, Leuven, Belgium (S.H., K.P., E.D.C., D.S.); The Panum Institute, Copenhagen, Denmark (L.-O.G.; T.W.S.); and AnorMed, Langley, British Columbia, Canada (G.B., G.H.)

Received December 19, 2000; accepted March 29, 2000

This paper is available online at http://molpharm.aspetjournals.org

ABSTRACT

The bicyclam AMD3100 is a highly potent and selective CXCR4 antagonist with strong antiviral activity against human immunodeficiency virus (HIV)-1 and HIV-2, which use CXCR4 as coreceptor for host cell entry. Here, we investigated the interaction of AMD3100 with CXCR4 at the molecular level by mutational analysis. We established a set of stably transfected U87.CD4 cell lines expressing different mutant forms of CXCR4 (i.e., CXCR4[WT], CXCR4[D171N], CXCR4[D262N], CXCR4[D171N,D262N], and CXCR4[H281A]), to compare the activity of the compound against mutated versus wild-type CXCR4. We found that the antagonistic action of AMD3100 against CXCR4—as assessed by the inhibitory effects of the compound on stromal cell-derived factor (SDF-1) binding to its receptor and on SDF-1-induced intracellular calcium signaling, and by displacement of the CXCR4-specific antibody, clone 12G5—was greatly reduced by substitution of Asp^{171} and/or Asp^{262} by neutral asparagine residue(s). Both aspartates, but most particularly Asp^{262}, also proved essential for the anti-HIV-1 activity of AMD3100 against the viruses NL4.3, IIIB, and HE. In contrast, substitution of His^{281} by a neutral alanine potentiated the antagonistic and antiviral effects of the compound in the different assay systems. Importantly, compared with the wild-type receptor, CXCR4[D262N] was much less effective, whereas CXCR4[D171N,D262N] completely failed as a coreceptor for infection by HIV-1 NL4.3. Thus, the negatively charged aspartate residues at positions 171 and 262, located in transmembrane domains 4 and 6 of the 7-transmembrane receptor, respectively, may represent crucial sites for electrostatic interaction of the positive charges of the bicyclams, as well as for the highly basic V3 loop of the gp120 envelope protein of certain HIV-1 strains.

The bicyclam AMD3100 (Fig. 1A) was originally described as a highly potent and selective inhibitor of HIV-1 and HIV-2 replication, active against a wide variety of T cell (T)-tropic but not macrophage (M)-tropic HIV strains (De Clercq et al., 1994; De Vreese et al., 1996). Only recently, the cellular tropism of HIV could be clarified by the discovery that, in addition to the CD4 receptor, one of the cellular chemokine receptors, CXCR4 or CCR5, is required as a cofactor for viral entry into the host cell (Berger et al., 1999). The chemokine receptors belong to the class of G protein-coupled 7-transmembrane receptors. CCR5 binds several CC-chemokine ligands [i.e., regulated upon activation normal T cell expressed and secreted (RANTES), macrophage inflammatory protein (MIP)-1α and MIP-1β], and is the main coreceptor for M-tropic HIV-1 strains (now indicated as R5 strains) (Alkhatib et al., 1996). These R5 viruses have been isolated from patients during the initial (asymptomatic) stage of the infection and are responsible for transmission of HIV infection between persons (Deng et al., 1996). CXCR4 (Fig. 1B) is the receptor for the CXC-chemokine stromal cell-derived factor-1 (SDF-1) (Bleul et al., 1996; Oberlin et al., 1996) and is used as coreceptor by the pathogenic T-tropic viruses (Feng et al., 1996; Connor et al., 1997) (now designated X4 strains) that emerge at a later stage of the disease and are responsible for the rapid decline in the CD4$^+$ T cell count and progression toward AIDS.

It has been shown by our group that the selective antiviral activity of AMD3100 against X4 HIV strains is based on the

S.H. is a Postdoctoral Research Assistant of the 'Fonds voor Wetenschappelijk Onderzoek (FWO)—Vlaanderen'. This work was supported by grants from the 'Fonds voor Wetenschappelijk Onderzoek (FWO)—Vlaanderen' (Krediet no. G.0104.98), and the 'Geconcerteerde Onderzoeksacties (Vlaamse Gemeenschap)' (Krediet 00/12).

ABBREVIATIONS: HIV, human immunodeficiency virus; SDF-1, stromal cell-derived factor-1; PBS, phosphate-buffered saline; FBS, fetal bovine serum; PE, phycoerythrin; mAb, monoclonal antibody; RT-PCR, reverse transcription polymerase chain reaction; LTR, long terminal repeat; TM, transmembrane domain; Ag, antigen; GAPDH, glyceraldehyde 3-phosphate dehydrogenase; WT, wild-type.

specific blockade of CXCR4-mediated virus entry via direct interaction of the compound with CXCR4. This could be demonstrated by the concentration-dependent inhibitory effects of AMD3100 on 1) the binding of the CXCR4-specific mAb 12G5 at the cell surface, 2) the binding of SDF-1 to the receptor, and 3) the intracellular calcium signal and chemotactic response elicited by SDF-1 (Schols et al., 1997b; Donzella et al., 1998). Because AMD3100 counteracts the effects of the natural receptor ligand SDF-1 without triggering any response by itself upon binding to the receptor (Schols et al., 1997b; Donzella et al., 1998), the compound has been defined as a pure and specific CXCR4 antagonist.

Inhibition of viral entry into the host cell by antagonization of CXCR4 and/or CCR5 represents an important new approach for anti-HIV therapy. Based on its promising antiviral efficacy in cell cultures and in the in vivo SCID-hu Thy/Liv model (Datema et al., 1996) and the SCID-hu PBMC model (D. Schols, unpublished observations), AMD3100 has recently entered clinical studies. A phase I trial unveiled no signs of toxicity (Hendrix et al., 2000), and the therapeutic potential of the compound is currently being evaluated in a phase II study with patients infected with HIV.

However, except for one study reported by Labrosse et al. (1998), the precise molecular interactions underlying the high-affinity binding of AMD3100 to CXCR4 have not yet been investigated in detail. AMD3100 consists of two macrocyclic polyamine cyclam [1,4,8,11-tetraazacyclotetradecane] units connected by an aromatic linker (Fig. 1A). The presence of eight amines is responsible for the net positive charge (+4) of the molecule. Remarkably, the natural CXCR4 ligand, SDF-1, and the V3 loop of X4 HIV gp120 are highly basic, and thus carry an overall positive charge as well (Dealwis et al., 1998). It is tempting to speculate that those positive charges play a role in the binding to the receptor, by electrostatic interaction with negatively charged amino acid residues, which are abundantly present in the extracellular regions of CXCR4 (net charge −9) (Fig. 1B and Dealwis et al., 1998).

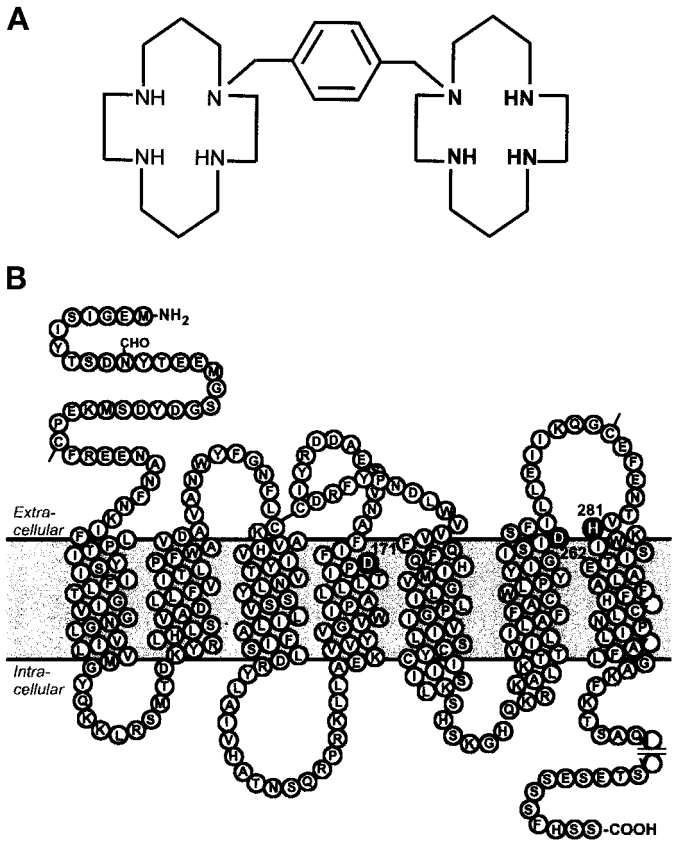

Fig. 1. A, chemical structure of the bicyclam AMD3100, 1,1′-[1,4-phenylenebis(methylene)]-bis-1,4,8,11-azatetradecane. B, amino acid sequence and membrane organization of the chemokine receptor CXCR4.

To investigate this possibility, a mutational analysis study has been undertaken to examine the impact of single amino acid substitutions in CXCR4 on the binding affinity of a series of mono- and bicyclam derivatives (Gerlach et al., 2001). This initial study showed that both Asp^{171} (in TM4) and Asp^{262} (in TM6), located at each end of the main ligand-binding crevice of the CXCR4 receptor, are essential for the high-affinity binding site of AMD3100 (Gerlach et al., 2001).

In the present study, we focused mainly on these two residues. We created stably transfected cell lines expressing CXCR4 variants in which one or both of these aspartates are replaced with a neutral asparagine residue. We also included in our study a CXCR4 mutant carrying a histidine-to-alanine substitution at position 281. His^{281} is located very near Asp^{262} (Fig. 1B) and thus may have important consequences for the electrostatic interaction between AMD3100 and CXCR4. We chose the CD4-transfected human astroglioma U87 cells (Bjorndal et al., 1997) to introduce the CXCR4 mutants, so that the resulting CD4/CXCR4 double-transfected cell lines could also be evaluated for HIV infection. We used these cell lines to demonstrate the necessity of Asp^{171} and Asp^{262} for the biological activity of AMD3100 as a CXCR4 antagonist and as an HIV entry inhibitor.

Materials and Methods

Viruses and Cell Cultures. The HIV-1 T-tropic (X4) molecular clone NL4.3 was obtained from the National Institute of Allergy and Infectious Disease AIDS reagent program (Bethesda, MD). The T-tropic HIV-1 IIIB strain was a kind gift from Dr. L. Montagnier (Pasteur Institute, Paris, France). The dual-tropic (R5/X4) HIV-1 HE strain was initially isolated from a patient at the University Hospital in Leuven and had been routinely cultured in MT-4 cells (Pauwels et al., 1990). Human astroglioma U87 cells expressing human CD4 (U87.CD4) (Bjorndal et al., 1997) were kindly provided by Dr. Dan R. Littman (Skirball Institute of Biomolecular Medicine, New York University Medical Center, New York, NY) and were cultured in Dulbecco's modified Eagle's medium (Invitrogen, Paisley, UK) containing 10% fetal bovine serum (FBS) (BioWhittaker Europe, Verviers, Belgium), 0.01 M HEPES buffer (Invitrogen), and 0.2 mg/ml geneticin (G-418 sulfate) (Invitrogen). The cell cultures were maintained at 37°C in a humidified, CO_2-controlled atmosphere and subcultivations were done every 2 to 3 days by digestion of the monolayers with trypsin (Invitrogen).

Compounds and Chemokines. The bicyclam AMD3100 was synthesized as described previously (Bridger et al., 1995). The CXC-chemokine SDF-1 was provided by Dr. I. Clark-Lewis (University of British Columbia, Vancouver, BC, Canada).

Plasmids. Single or double amino acid substitutions in CXCR4 were achieved by site-directed mutagenesis. The point mutations were introduced in the coding sequence of the receptor by the polymerase chain reaction (PCR) overlap extension technique (Ho et al., 1989) using the human wild-type CXCR4 cDNA as template. All reactions were carried out using the *Pfu* polymerase (Stratagene, La Jolla, CA) under conditions recommended by the manufacturer. The generated fragments were subcloned into the pTEJ-8 eukaryotic expression vector (Johansen et al., 1990) containing the wild-type

CXCR4 cDNA under the control of the strong and constitutive human ubiquitin promoter, by substituting the wild-type cDNA fragment with the mutated cDNA fragment. The mutations were verified by restriction endonuclease digestion and DNA sequencing (ABI310; PerkinElmer Life Science Products, Boston, MA).

Construction of Stably Transfected Cell Lines. The pTEJ-8 expression vectors encoding the different forms of CXCR4 were cotransfected with the pPUR selection vector encoding puromycin resistance (CLONTECH Laboratories, Palo Alto, CA) into U87.CD4 cells by the use of FuGENE 6 Transfection Reagent (Roche Molecular Biochemicals, Mannheim, Germany) according to the manufacturer's instructions. Puromycin (1 μg/ml) selection was started after 18 h. After approximately 3 weeks, nicely growing puromycin-resistant cell cultures, containing 10 to 30% CXCR4-positive cells (as determined by flow cytometry; see below), were established for each of the CXCR4 variants. CXCR4-expressing cells were isolated from these cell cultures as follows. Approximately 4×10^6 cells in 500 μl of PBS containing 2% FBS were incubated with 20 μl of nonconjugated mouse anti-human CXCR4 antibody clone 12G5 (BD PharMingen, San Diego, CA) for 30 min at room temperature. After two washing steps, the cells were incubated with 2×10^6 sheep anti-mouse IgG-conjugated Dynabeads M450 (Dynal, Oslo, Norway) in 8 ml of PBS with 2% FBS for 1 h at 4°C under continuous gentle rotation. Thereafter, the CXCR4-positive cells (which had bound magnetic beads at their surface) were isolated from the cell suspension by magnetic separation and were thoroughly washed with PBS and transferred to puromycin-containing growth medium.

RT-PCR analysis of CXCR4 expression. Total RNA was isolated from approximately 2×10^6 cells using the RNeasy Mini Kit (QIAGEN, Hilden, Germany). To eliminate any possible contamination by genomic DNA, DNase treatment (RNase-free DNase Set, QIAGEN) was included in the RNA purification protocol. The RNA concentration of the samples was determined spectrophotometrically at 260 nm. After a 1-min denaturation at 95°C, 2 μg of RNA was reverse transcribed by 4 U of Rous-associated virus (RAV-2) reverse transcriptase (Amersham-Pharmacia Biotech, Uppsala, Sweden) in a 50-μl mixture consisting of reaction buffer (supplied with the enzyme) with 250 μM concentrations of each dATP, dGTP, dCTP, and dTTP (Invitrogen), 6 μg of random hexanucleotide primers (Invitrogen) and 130 U of human placental ribonuclease inhibitor (Amersham-Pharmacia Biotech). The reaction was allowed to proceed for 90 min at 45°C, whereafter the cDNA samples were stored frozen until the CytoXpress Multiplex PCR kit for detection of human CXC-chemokine receptors (BioSource, Camarillo, CA) was used according to the manufacturer's instructions. PCR products were electrophoresed through a 2% agarose gel and visualized by ethidium bromide. The bands were quantified by densitometry (Image Master software) and the intensity of the CXCR4 band was normalized to that of the coamplified GAPDH fragment.

Flow Cytometry. The antibodies used in this study were: mouse anti-human CXCR4 mAb clone 12G5 (unconjugated, BD PharMingen; PE-conjugated, R&D Systems Europe, Oxon, United Kingdom), mouse anti-human CXCR4 mAb clone 173 (R&D Systems Europe, Abingdon, Oxon, UK), rat anti-human CXCR4 clone 2B11 (kindly provided by Dr. R. Förster, Max Delbrück Center for Molecular Medicine, Berlin-Buch, Germany), fluorescein isothiocyanate-conjugated goat anti-mouse IgG Ab and fluorescein isothiocyanate-conjugated goat anti-rat IgG Ab (Caltag Laboratories, San Francisco, CA).

After trypsin digestion, CXCR4-transfected U87.CD4 cells were incubated for at least 1 h at room temperature to allow re-expression of receptor proteins at the cell surface. Then, 0.5×10^6 cells were washed once with PBS containing 2% FBS, resuspended in 100 μl PBS containing 2% FBS, and incubated with anti-CXCR4 antibody for 30 min on ice. Thereafter, the cells were washed and, in case of an unlabeled primary antibody, incubated for 30 min on ice with the appropriate secondary antibody (diluted 1/100 in PBS with 2% FBS). After final washing with PBS, the cell samples were fixed in 1% paraformaldehyde in PBS and analyzed on a FACScan flow cytometer (Becton Dickinson, San Jose, CA). As a negative control for aspecific background staining, the cells were stained in parallel with Simultest Control γ_1/γ_{2a} (Becton Dickinson) (for PE-conjugated anti-CXCR4 12G5 mAb) or with the corresponding secondary antibody alone (for the nonconjugated anti-CXCR4 12G5, 173 and 2B11 mAbs).

To evaluate the effect of AMD3100 on 12G5 mAb binding at the cell surface, the cells were preincubated with AMD3100 in PBS for 15 min at room temperature and washed once with PBS with 2% FBS before incubation with PE-conjugated anti-CXCR4 (12G5) mAb.

Measurement of Intracellular Calcium Mobilization. On the day before the experiment, the U87.CD4.CXCR4 transfectants were seeded in 0.1% gelatin-coated, 96-well, black-wall microplates (Costar, Cambridge, MA) at 2×10^4 cells per well. On the day of the experiment, the cells were loaded with the fluorescent calcium indicator Fluo-3 acetoxymethyl ester (Molecular Probes, Leiden, The Netherlands) at 4 μM for 45 min at 37°C. After thorough washing with calcium flux assay buffer (Hanks' balanced salt solution with 20 mM HEPES buffer and 0.2% bovine serum albumin, pH 7.4), the cells were preincubated for 10 min at 37°C with AMD3100 at different concentrations in the same buffer. Then, the intracellular calcium mobilization in response to 2 ng/ml (for U87.CD4.CXCR4[WT]), 10 ng/ml (for U87.CD4.CXCR4[D171N] and -[D262N]), or 50 ng/ml (for U87.CD4.CXCR4[D171N,D262N] and -[H281A]) SDF-1 was measured at 37°C by monitoring the fluorescence as a function of time simultaneously in all the wells using a Fluorometric Imaging Plate Reader (FLIPR) (Molecular Devices, Sunnyvale, CA).

HIV Entry PCR. The U87.CD4.CXCR4 cell variants were seeded in 24-well plates at 5×10^4 cells per well and incubated overnight. Virus stocks (diluted to a p24 titer of 10,000 pg/ml) were treated with 500 U/ml of RNase-free DNase (Roche Molecular Biochemicals) for 1 h at room temperature. Then, the cells in each well were infected with 1000 pg of p24. To control for possible residual contamination of the viral inoculum with viral DNA, a parallel infection was carried out on the nontransfected (CXCR4-negative) U87.CD4 cells. After incubation at 37°C for 2 h, the medium was aspirated, the cells were washed once with PBS, and total DNA was extracted from the infected cells using the QIAamp DNA Mini Kit (QIAGEN). The DNA was eluted from the QIAamp spin columns in a final volume of 250 μl of elution buffer. Then, 5 μl of each DNA sample was subjected to 35 cycles of HIV-1 LTR R/U5-specific and 30 cycles of β-actin-specific PCR on a T3 Thermocycler (Biometra, Göttingen, Germany). Each cycle comprised a 45-s denaturation step at 95°C, a 45-s annealing step at 61°C and a 45-s extension step at 72°C. The primers used were: LTR R/U5 sense primer 5′-GGCTAACTAGGGAACCCACTG-3′ (nucleotides 496 to 516, according to the HIV-1 HXB-2 DNA sequence; see Ratner et al., 1985), LTR R/U5 antisense primer 5′-CTGCTAGAGATTTTCCACACTGAC-3′ (nucleotides 612 to 635), β-actin sense primer 5′-TCTGGCGGCACCACCATGTACC-3′ (nucleotides 2658 to 2679), β-actin antisense primer 5′-CGATGGAGGGGCCGGACTCG-3′ (nucleotides 2961 to 2980). The reaction mixtures contained PCR buffer (supplied with the enzyme), 200 μM concentrations of each dATP, dGTP, dCTP and dTTP (Invitrogen), 0.4 μM concentrations of each of the forward and reverse primers, and 0.5 U of SuperTaq DNA polymerase (HT Biotechnology, Cambridge, England) in a total volume of 25 μl. After gel electrophoresis through a 2% agarose gel, the amplified DNA fragments were visualized by ethidium bromide. In preliminary experiments, the exponential range of the PCR amplification curve was determined for both the HIV-1 LTR R/U5 and the β-actin PCRs by varying the amount of input DNA and the number of PCR cycles. Based on these experiments, appropriate conditions were chosen to perform the PCRs. In the experiments, linearity was ascertained for each sample by running parallel PCRs on 2.5 μl instead of 5 μl of input DNA.

Antiviral Activity Assay. The U87.CD4.CXCR4 transfectants were seeded in 24-well plates (2×10^4 cells per well in 1 ml of culture medium) and preincubated for 15 min with AMD3100 at different

concentrations. Then, 1000 pg/ml p24 Ag of the different HIV-1 strains was added.

The cytopathic effect of virus replication in the cell cultures (syncytium formation) was evaluated microscopically at day 4 to 7 after infection. Also, culture supernatants were collected at day 5 and analyzed for HIV-1 core antigen by p24 Ag ELISA (DuPont-Merck Pharmaceutical Co., Wilmington, DE), and the IC_{50} value of AMD3100 (i.e., the 50% inhibitory concentration for virus replication) was calculated.

Results

Construction of Stably Transfected Cell Lines Expressing Different CXCR4 Mutants and Evaluation of CXCR4 Expression. Stably transfected U87.CD4 cell lines expressing CXCR4 variants with different mutations (i.e., D171N; D262N; D171N, D262N, and H281A) were constructed and designated U87.CD4.CXCR4[WT], U87.CD4.CXCR4[D171N], U87.CD4.CXCR4[D262N], U87.CD4.CXCR4[D171N,D262N], and U87.CD4.-CXCR4 [H281A], respectively. The H281A substitution was included in our study because it eliminates a charged amino acid (i.e., His^{281}), which is located very close to Asp^{262} (see Fig. 1B).

The CXCR4 expression of the transfectants was analyzed at both the mRNA and the protein levels. As shown in Fig. 2A, RT-PCR with GAPDH as an internal reference control did not reveal significant differences in CXCR4 mRNA levels between the five cell lines: the ratios of CXCR4 to GAPDH band intensity ranged only between 0.42 and 0.59.

The CXCR4 protein expression at the cell membrane was analyzed flow-cytometrically with different antibodies recognizing distinct CXCR4 epitopes. None of the antibodies used showed any positive staining on the parental (non-CXCR4-transfected) U87.CD4 cells (Fig. 2B). Reactivity with the 12G5 mAb, which interacts with the second extracellular loop of CXCR4, was markedly decreased in U87.CD4.CXCR4-[D171N], U87.CD4.CXCR4[D171N, D262N], and U87.CD4. CXCR4[H281A] cells, compared with U87.CD4.CXCR4[WT] and U87.CD4.CXCR4[D262N] cells (Fig. 2B). The respective mean fluorescence intensity values of the cell populations for CXCR4-specific staining by 12G5 were 26, 19, and 12 versus 46 and 58. In contrast, staining with the anti-CXCR4 2B11 mAb, which recognizes an epitope in the amino-terminal domain of the receptor molecule (Förster et al., 1998), revealed comparable CXCR4 expression levels in all five cell lines (Fig. 2B). Here, the mean fluorescence intensities for CXCR4-specific staining varied between 13 and 18. In addition, adequate cell surface expression of the different CXCR4 mutants was also verified by the CXCR4-specific 173 mAb, yielding mean fluorescence intensities of 188, 156, 260, 161 and 78 for U87.CD4.CXCR4[WT], U87.CD4.CXCR4[D171N], U87.CD4.CXCR4[D262N], U87.CD4.-CXCR4[D171N, D262N], and U87.CD4.CXCR4[H281A] cells, respectively (Fig. 2B).

Antagonistic Activity of AMD3100 against the Different CXCR4 Mutants. The effect of the different amino acid substitutions on the antagonistic properties of AMD3100 against CXCR4 was examined by evaluating the ability of the compound to block SDF-1-induced calcium signaling in the respective transfected cell lines.

In all five cell lines, SDF-1 elicited a dose-dependent intracellular calcium flux, although the chemokine concentrations required to yield responses of comparable magnitude differed among the CXCR4 variants. Therefore, U87.CD4.CXCR4[WT] cells were stimulated with 2 ng/ml SDF-1, while a chemokine concentration of 10 ng/ml had to be applied on U87.CD4.CXCR4[D171N] and U87.CD4.CXCR4[D262N] cells and 50 ng/ml on U87.CD4.CXCR4[D171N,D262N] and U87.CD4.CXCR4[H281A] cells.

To investigate the antagonistic activity of AMD3100, the cells were preincubated for 10 min with different compound concentrations, whereafter they were triggered with the appropriate concentrations of SDF-1. In U87.CD4.CXCR4[WT] and U87.CD4.CXCR4[H281A] cells, pretreatment with AMD3100 at 1 μg/ml totally abrogated the calcium response (Fig. 3A). In contrast, only a minor reduction in responsiveness to SDF-1 could be observed in U87.CD4.CXCR4[D171N] and U87.CD4.CXCR4[D262N] cells after pretreatment with 1 μg/ml AMD3100, whereas at this concentration, the compound completely failed to block the intracellular calcium flux in U87.CD4.CXCR4[D171N,D262N] cells (Fig. 3A). Figure 3B shows the concentration-dependent inhibition of SDF-1-induced calcium flux by AMD3100. The IC_{50} values, as estimated by semilogarithmic interpolation, were approximately 100, 2,700, 7,500, 25,000 and 50 ng/ml for CXCR4[WT], CXCR4[D171N], CXCR4[D262N], CXCR4[D171N,D262N], and CXCR4[H281A], respectively. Thus, replacement of the aspartic acids at positions 171 and/or 262 by asparagine severely affected the antagonistic activity of AMD3100.

Inhibition of 12G5 Binding to the CXCR4 Mutants by AMD3100. To examine the impact of the different mutations on the inhibitory activity of AMD3100 against 12G5 mAb binding at the cell surface, the different U87.CD4.CXCR4 transfectants were preincubated during 15 min with AMD3100 at 1 μg/ml, whereafter the compound was washed away and the binding of PE-conjugated 12G5 mAb was measured by flow cytometry. The amount of 12G5 mAb bound to the cells was estimated by the mean fluorescence intensity of the cells. After exposure to AMD3100, antibody binding had decreased by 88, 20, 9, 9, and 98% compared with the respective untreated control cells, for U87.CD4.CXCR4[WT], U87.CD4.CXCR4[D171N], U87.CD4.CXCR4[D262N], U87.CD4.CXCR4-[D171N,D262N], and U87.CD4.CXCR4[H281A] cells, respectively (Fig. 4). Thus, AMD3100 substantially lost its blocking capacity on 12G5 mAb binding for the D171N and D262N mutants and the D171N, D262N double mutant. On the other hand, H281A substitution resulted in a slightly increased activity of the compound (Fig. 4). These data are in line with the results obtained with the calcium mobilization assays.

Coreceptor Function of the CXCR4 Mutants for HIV-1 Entry. To find out whether the D171N, D262N and H281A mutations have any influence on the HIV coreceptor function of CXCR4, we performed a semiquantitative HIV-1 LTR R/U5-specific PCR on total DNA isolated from the different transfectants at 2 h after infection with either the X4 strain NL4.3 or the R5/X4 dual-tropic strain HE. Synthesis of the LTR R/U5 DNA transcript, also known as 'strong-stop DNA', is the first step of the reverse transcription process and is accomplished at a very early stage of the infection, immediately after viral entry and uncoating.

As shown in the left panel of Fig. 5, CXCR4[D171N] and CXCR4[H281A] were equally efficient as CXCR4[WT] in mediating NL4.3 entry. In contrast, D262N substitution negatively affected the coreceptor function of CXCR4 for

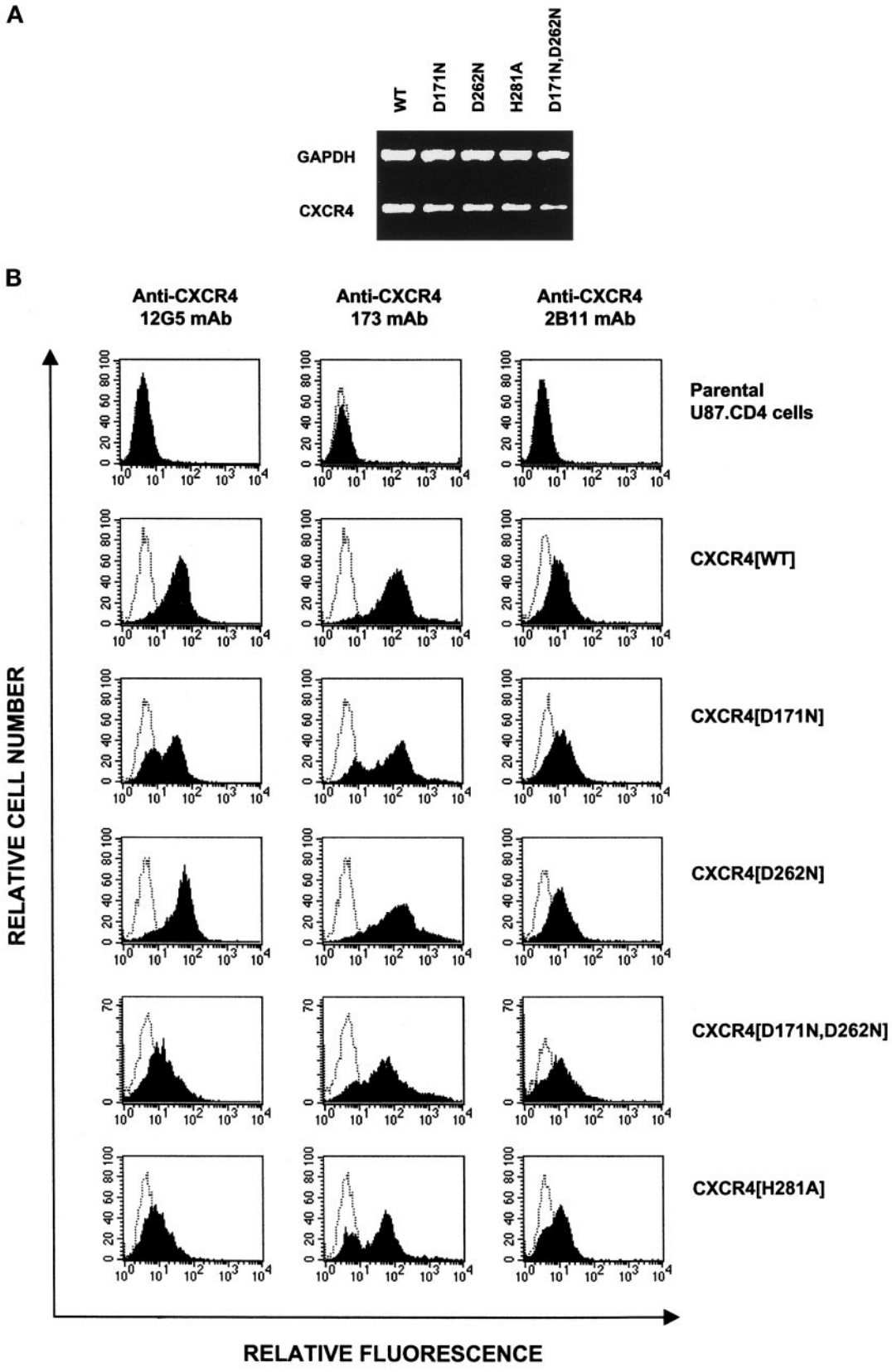

Fig. 2. A, RT-PCR analysis of CXCR4 mRNA levels in the stably transfected U87. CD4 cells expressing the different CXCR4 variants. GAPDH was coamplified as an internal reference. The ratios of CXCR4 band intensity to the respective GAPDH band intensity were determined by densitometric analysis. B, flow cytometric analysis of the membrane expression of CXCR4 in the stably transfected cell lines. The black curves represent CXCR4-specific staining by the 12G5 mAb (left), reacting with an epitope located in ECL2, by the 173 mAb (middle), or by the 2B11 mAb (right), directed against the amino-terminal domain of CXCR4. The white histograms represent the background fluorescence caused by aspecific binding of the respective secondary antibodies.

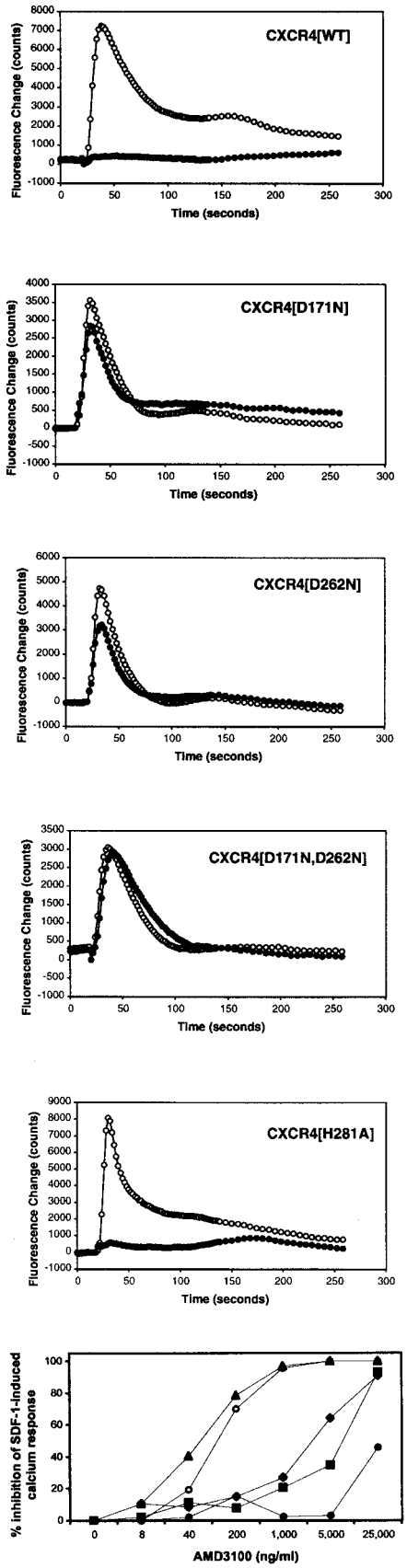

Fig. 3. Inhibition of SDF-1-induced intracellular calcium mobilization by AMD3100 in the different transfectants. After loading with the fluorescent calcium indicator Fluo-3, the cells were preincubated for 10 min with or without compound and were then stimulated with the chemokine at 2, 10, or 50 ng/ml depending on the cell line (see *Materials and Methods*). The transient increase in the intracellular calcium concentration was recorded by monitoring the change in fluorescence of the cells as a function of time using the Fluorometric Imaging Plate Reader (FLIPR). Top five graphs, SDF-1-induced calcium flux in the absence of AMD3100 (open symbols) or after preincubation of the cells with AMD3100 at 1 μg/ml (closed symbols). Each data point represents the mean fluorescence of quadruplicate microplate wells. The data of one experiment representative of four are shown. Bottom graph, concentration-dependence of the antagonistic activity of AMD3100. ○, CXCR4[WT]; ■, CXCR4[D262N]; ▲, CXCR4[H281A]; ♦, CXCR4[D171N]; ●, CXCR4[D171N,D262N].

NL4.3, and no viral DNA at all could be detected in U87.CD4.CXCR4[D171N,D262N] cells.

In accord with these data, microscopic evaluation of the cell cultures at day 5 after infection (Fig. 6A) revealed comparable strong cytopathic effects of NL4.3 on the CXCR4[WT]-, CXCR4[D171N]-, and CXCR4[H281A]-transfectants, although the extent of giant cell formation was markedly reduced in the U87.CD4.CXCR4[D262N] cells. In U87.CD4.CXCR4[D171N, D262N] cells, no visible signs of virus infection could be observed (Fig. 6A). Quantification of the viral p24 core Ag in the supernatants of the infected cell cultures confirmed the microscopic observations (Fig. 6B). Within each independent experiment, p24 Ag production varied less than 3-fold between NL4.3-infected U87.CD4.CXCR4[WT], U87.CD4.CXCR4-[D171N], and U87.CD4.CXCR4[H281A] cells, whereas the p24 Ag levels were consistently >40-fold lower in U87.CD4.CXCR4[D262N] cells and below the detection limit (i.e., 5 pg/ml) for U87.CD4.CXCR4[D171N,D262N] cells (Fig. 6B). Similar observations were made with the HIV-1 IIIB strain (data not shown).

The HIV-1 HE strain on the other hand yielded a different picture for viral replication. Based on the PCR assay, each of the four CXCR4 mutants proved somewhat less effective as a coreceptor for viral entry than the wild-type receptor (Fig. 5, right). However, after 4 days of infection with the HE strain, no significant differences in viral replication could be observed, either microscopically (data not shown) or by p24 Ag measurements (Fig. 6B), between the mutants and the wild-type receptor.

Antiviral Activity of AMD3100 in the U87.CD4.CXCR4 Cell Lines. Table 1 displays the IC_{50} values of AMD3100 for replication of HIV-1 NL4.3, IIIB, and HE in the wild-type versus mutant CXCR4-transfected U87.CD4 cells. Consistent with our previous antiviral studies with AMD3100 (Schols et al., 1997a), the compound strongly inhibited HIV-1 replication in U87.CD4.CXCR4[WT] cells, the IC_{50} value being ~10 ng/ml for all virus strains (Table 1). At 40 ng/ml, the compound totally blocked viral replication (data not shown). Compared with the wild-type CXCR4-expressing cells, a 2- to 4-fold increase in IC_{50} was noted for both X4 strains, NL4.3, and IIIB, in U87.CD4.CXCR4[D171N] cells. For the R5/X4 strain HE, the negative effect of the D171N mutation on the antiviral activity of AMD3100 was more pronounced (>30-fold increase in IC_{50} value compared with the wild-type receptor) (Table 1). Substitution of Asp^{262} resulted in a 7-, >20-, and >80-fold decrease in antiviral potency of AMD3100 against NL4.3, IIIB, and HE replication, respectively (Table 1). In the U87.CD4 cells expressing the double mutant form of CXCR4, the IC_{50} of AMD3100 for NL4.3 and IIIB replication could not be determined, because virus production was consistently below the detection limit in the positive (untreated) virus control (data described above). For

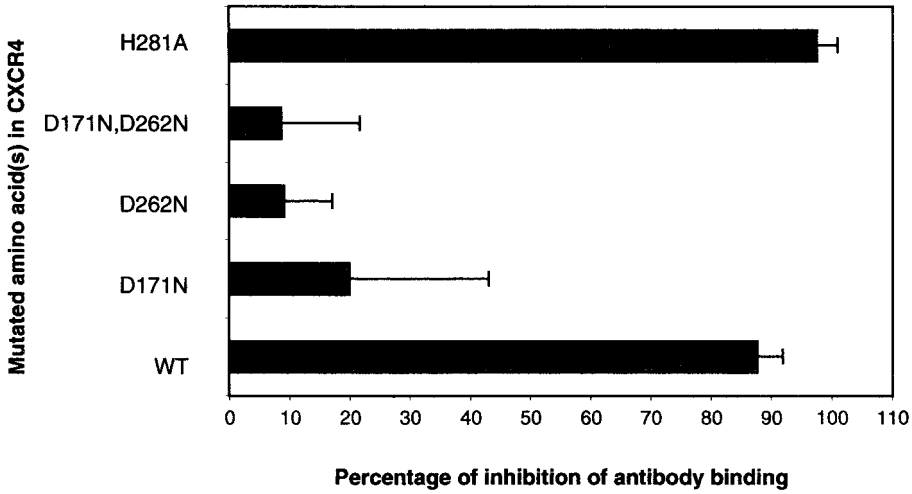

Fig. 4. Inhibition of 12G5 mAb binding to the different CXCR4 mutants by AMD3100. The stably transfected U87.CD4.CXCR4 cells were treated for 15 min with AMD3100 at 1 μg/ml and were then stained with PE-conjugated 12G5 mAb and analyzed by flow cytometry. An isotype control mAb was used to correct for aspecific staining. The mean fluorescence intensity in the untreated positive control of each cell line was set equal to 100% (no inhibition of 12G5 binding). Antibody binding in the AMD3100-treated cell samples was expressed as a percentage of the corresponding positive control, and the percentage of inhibition was calculated. The bars represent the mean ± S.D. of three independent experiments.

the HE strain, the IC_{50} could be determined and there was a >80-fold loss of antiviral activity of AMD3100 in this cell line, compared with the U87.CD4.CXCR4[WT] cells (Table 1). The data in Table 1 also show that D262N substitution had a larger impact on the antiviral activity of AMD3100 than D171N replacement. On the other hand, AMD3100 became approximately 10-fold more active against NL4.3IIIB, and HE replication in U87.CD4.CXCR4[H281A] compared with U87.CD4.CXCR4[WT] cells (Table 1). In the U87.CD4.CXCR4-[H281A] cell line, virus production was completely suppressed by AMD3100 at a concentration as low as 8 ng/ml for both NL4.3 and HE (data not shown).

Discussion

In this study, we provide evidence that the two aspartic acid residues at positions 171 and 262 of the chemokine receptor CXCR4 are indispensable for the strong and specific interaction of the bicyclam AMD3100 with the receptor protein. Single or combined substitution of these aspartates by neutral asparagines resulted in a markedly decreased potency of AMD3100 for inhibition of 1) SDF-1 binding to the receptor, 2) SDF-1-induced intracellular calcium signaling, 3) anti-CXCR4 12G5 mAb binding at the cell surface, and 4) viral entry into the cells by the CXCR4-using HIV-1 strains NL4.3, IIIB, and HE.

With regard to the calcium mobilization assays, it may be worth mentioning that different chemokine concentrations had to be applied onto the different transfectant cells to elicit comparable calcium responses. Particularly, a 25-fold higher SDF-1 dose afforded a 2-fold lower calcium flux in the double mutant, compared with the wild-type. This may point to altered SDF-1 binding to the CXCR4 mutants and/or changes in the signal transduction properties of the mutant compared with the wild-type receptors. The mutant receptors indeed showed a slightly lower SDF-1 affinity in the receptor binding assays (Gerlach et al., 2001).

The markedly reduced binding of anti-CXCR4 12G5 mAb to CXCR4[D171N], CXCR4[D171N,D262N], and CXCR4[H281A], but not CXCR4[D262N], suggests that the D171N and H281A mutations, unlike D262N, disrupt the 12G5 binding epitope. Given the fact that 12G5 mAb recognizes an epitope in ECL2, and because Asp^{171} is located in the close proximity of this domain (see Fig. 1B), the dramatic effect of D171N substitution on 12G5 mAb binding is not surprising. Moreover, the competition between AMD3100 and 12G5 mAb for binding to wild-type CXCR4 (Schols et al., 1997a,b; data presented herein) indicates that AMD3100 at least partly masks the 12G5 mAb recognition site. This is in agreement with our present finding that substitution of Asp^{171}, which was identified as a crucial interaction site for AMD3100, also affects the binding of 12G5 mAb. In addition, it has previously been reported that mutations in ECL2 and TM4, where Asp^{171} is located, mostly affect the reactivity of CXCR4 with 12G5 mAb, either by disrupting the 12G5 mAb binding epitope or by modifying its accessibility (Labrosse et al., 1998). On the other hand, the effect of the H281A mutation on 12G5 mAb binding is less obvious, but could possibly result from a slight modification of the global three-dimensional structure of the receptor protein, because the 12G5 mAb binding epitope is known to be conformation-dependent (Endres et al., 1996).

Interestingly, we found that viral infection by the X4 virus strains NL4.3 and IIIB was strikingly less efficient in U87.CD4.CXCR4[D262N] compared with U87.CD4.CXCR4[WT] cells. These viruses even completely failed to enter and infect U87.CD4.CXCR4[D171N,D262N] cells. Yet, U87.CD4.CXCR4 [D262N] and U87.CD4.CXCR4[D171N,D262N] cells showed a CXCR4 expression level comparable with that of U87.CD4.CXCR4[WT] cells. This was verified at the mRNA level by RT-PCR and at the protein level by flow cytometric analysis, using several CXCR4-specific mAbs, including one directed against an epitope in the amino-terminal region of

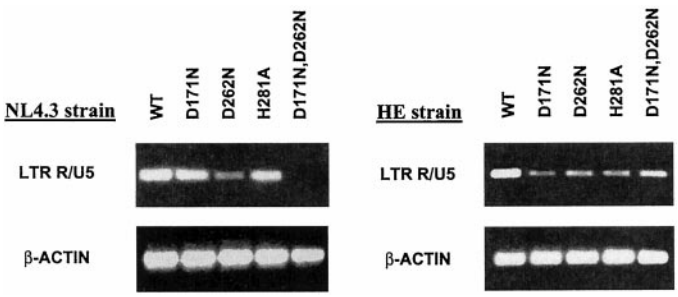

Fig. 5. PCR-based detection of virus entry into the U87. CD4 transfectants expressing the different CXCR4 mutants. Two hours after infection with HIV-1 NL4.3 or HIV-1 HE, total DNA was extracted from the cells and analyzed by semiquantitative PCR using HIV-1-specific primers from the LTR R/U5 region. DNA samples from mock-infected cells produced no signal (data not shown). DNA recovery was controlled by PCR with β-actin-specific primers. The results shown are from one representative experiment.

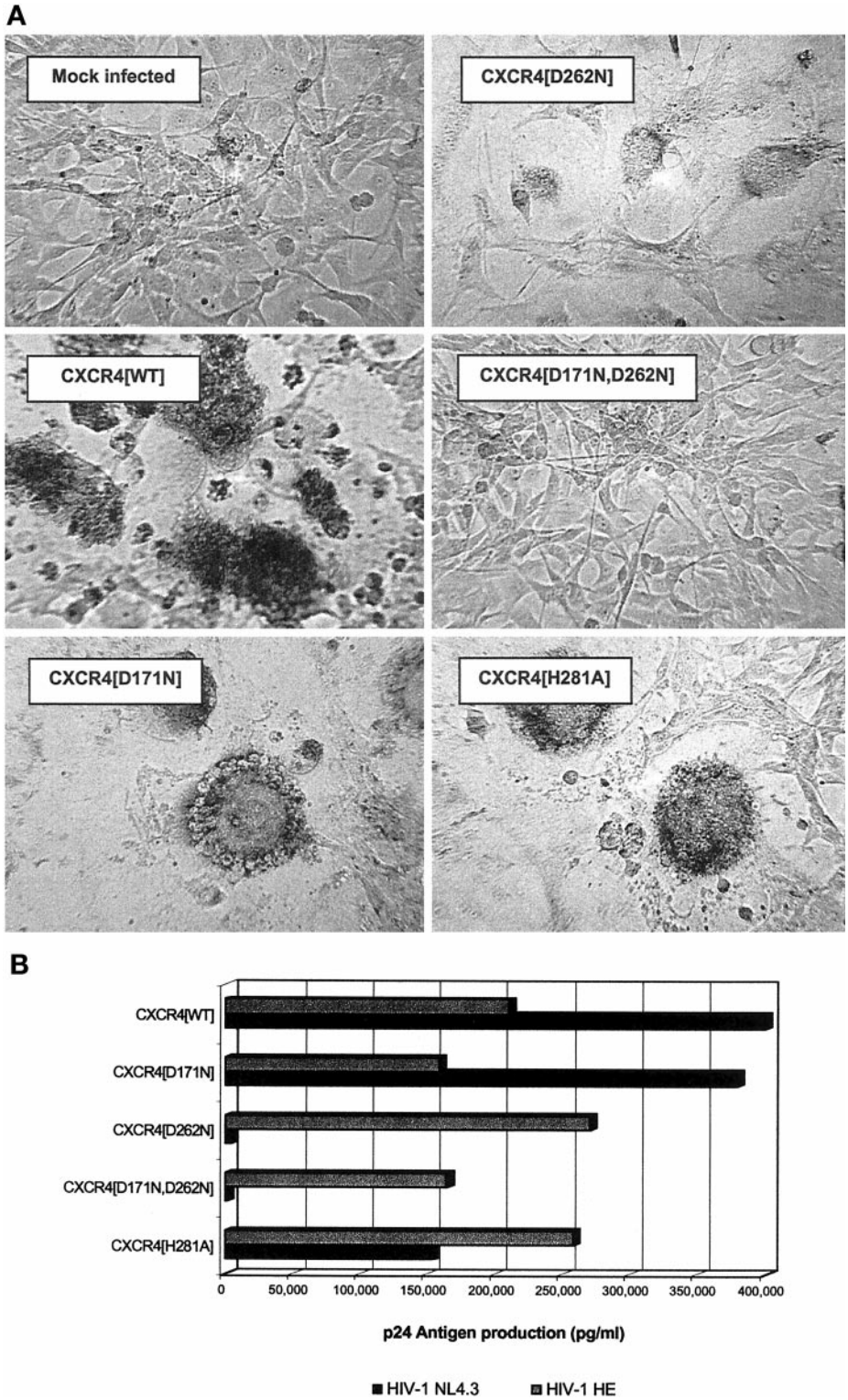

Fig. 6. A, cytopathic effect (giant cell formation) at day 5 after infection of the different U87.CD4.CXCR4 cell variants with HIV-1 NL4.3. Note the manifest syncytium formation in the U87.CD4.CXCR4[WT], U87.CD4.CXCR4[D171N], and U87.CD4.CXCR4[H281A] cell cultures, which is significantly less pronounced in the U87.CD4.CXCR4[D262N] and totally absent in the U87.CD4.CXCR4[D171N,D262N] cell cultures. Mock-infected U87.CD4.CXCR4[WT] cells are shown as a negative control. Similar images were obtained in several repeat experiments. B, viral core p24 Ag production by HIV-1 NL4.3- and HIV-1 HE-infected U87.CD4.CXCR4[WT], U87.CD4.CXCR4[D171N], U87.CD4.CXCR4[D262N], U87.CD4.CXCR4[D171N,D262N], and U87.CD4.CXCR4-[H281A] cell cultures. The p24 Ag enzyme-linked immunosorbent assays were performed on cell culture supernatants collected at day 6 after infection with the NL4.3 strain and at day 4 after infection with the HE strain. The results represent the mean of at least two independent experiments.

the receptor protein. Importantly, the level of CD4 expression was identical in all five CXCR4-transfected cell lines, as ascertained by flow cytometry (data not shown). Also, at the initial stage of infection, each of the CXCR4 mutants seemed to be less effective than the wild-type receptor in mediating viral entry of the R5/X4 HIV-1 HE strain. However, after 4 days of infection, these differences in coreceptor function were no longer detectable, which may be explained by the high cytopathogenicity of the HE strain. Thus, our observations indicate that Asp^{171} and, more particularly, Asp^{262} of the chemokine receptor CXCR4 also play an important role in the interaction between gp120 of certain CXCR4-using HIV-1 strains with the coreceptor. Moreover, Asp^{262} was also reported by Brelot et al. (2000) to be involved in the interaction with HIV-1 gp120. It is not known to date whether such mutant forms of CXCR4 also exist in vivo. If so, this might have important implications for the relative susceptibilities of different individual organisms to certain virus strains, as well as for the pathogenesis of AIDS in terms of coreceptor switch (Connor et al., 1997).

It should be noted that the relative importance of Asp^{171} and Asp^{262} for the activity of AMD3100 differed in the antiviral experiments compared with the chemokine binding, calcium mobilization, and antibody binding assays. The effect of the D171N mutation on the inhibitory activity of AMD3100 against NL4.3 and IIIB virus replication seemed to be surprisingly weak in comparison with the dramatic consequences of this mutation for the activity of the compound in the other (virus-free) assay systems. One possible explanation for this discrepancy may be that in the context of HIV infection, more complex molecular interactions (Atchison et al., 1996), involving CD4 as an additional participant, take place at the cell surface. Indeed, the initial binding of HIV gp120 to CD4 induces a conformational change in the gp120 complex, allowing it to interact with CXCR4 (Chan and Kim, 1998). This might at the same time influence the three-dimensional folding of CXCR4, which has been reported to colocalize with CD4 at the cell surface (Iyengar et al., 1998; Lapham et al., 1999). AMD3100 may interact with such gp120/CD4/CXCR4 complexes in a different way than with nonassociated CXCR4. Hence, it cannot be excluded that AMD3100 also uses alternative interaction sites (for example, the aspartates at positions 181, 182 or 193) to block the HIV coreceptor function of CXCR4. In support of this, Asp^{181}, Asp^{182}, and Asp^{193} were picked up as possible determinants for sensitivity to AMD3100 in the HIV fusion assays of Labrosse et al. (1998).

A remarkable phenomenon that was observed throughout all the different experiments was the beneficial effect of H281A substitution on the efficacy of AMD3100. This was most pronounced for the antiviral activity of the compound, which increased by approximately 10-fold in U87.CD4.CXCR4[H281A] compared with U87.CD4.CXCR4[WT] cells. Replacement of His^{281}, which is located close to the Asp^{262} interaction site (Fig. 1B), with a neutral alanine might potentiate the binding of AMD3100 to Asp^{262} by eliminating the electrostatic repulsion between the positive charges of the histidine residue in CXCR4, on the one hand, and the cyclam unit of AMD3100, on the other hand.

Our data suggest a model for binding of AMD3100 to the chemokine receptor in which the net positive charge of one cyclam unit of the compound interacts with the negatively charged aspartate at position 171 of CXCR4, and the other cyclam interacts with Asp^{262}. In this way, the compound occupies two interaction sites that are also indispensable for the NL4.3 virus strain, which was found unable to enter cells expressing the double mutant CXCR4[D171N,D262N]. This may help clarifying the outstanding potency of AMD3100 (ng/ml range) as an antiviral drug.

For wild-type CXCR4, AMD3100 showed equal IC_{50} values against the NL4.3 and HE virus strains. However, our PCR-based virus entry assays revealed a different profile of sensitivity to the mutations in the receptor protein for both virus strains. Moreover, the D171N substitution provoked a >30-fold decrease in the antiviral activity of AMD3100 against the HE strain but only a 2- to 4-fold reduced activity against NL4.3 and IIIB. These observations suggest that CXCR4-mediated viral entry of HE virus particles occurs via different gp120/CXCR4 interaction mechanisms than is the case for IIIB and NL4.3 virions. This is in agreement with a recent report by Kajumo et al. (2000) describing the varying dependence of different viral isolates on residues in one or another domain of CXCR4. In this regard, the consistent potent activity of AMD3100 against such a wide variety of X4 and R5/X4 virus strains or clinical isolates (De Clercq et al., 1994) is quite puzzling. Apparently, the high-affinity interaction of AMD3100 with particular amino acid residues of CXCR4, such as Asp^{171} and Asp^{262}, may also have an indirect, global negative effect on the coreceptor function of CXCR4 for virus strains entering the cells via distinct or even nonoverlapping coreceptor domains.

In conclusion, we have demonstrated by site-directed mutagenesis the crucial involvement of the two aspartate residues at positions 171 and 262 of the chemokine receptor CXCR4 in the high-affinity binding of the bicyclam AMD3100 to CXCR4. In addition, these two residues also emerged from this study as important determinants for the coreceptor activity of CXCR4 for certain HIV strains. Our new insights in the molecular interactions of AMD3100 with the receptor protein may help in the design of novel high-potency CXCR4 antagonists. Because the significance of CXCR4 and other CC- and CXC-chemokine receptors for other immune-related pathologies have only begun to be discovered (Murdoch and Finn, 2000), such receptor antagonists may be valuable drug candidates, not only for the treatment of HIV infections, but also in other fields of medicine, such as inflammation and allergy.

TABLE 1
IC_{50} values of AMD3100 for HIV-1 replication in the different U87.CD4.CXCR4 transfectants

CXCR4 Mutant	IC_{50}[a]		
	NL4.3 strain	IIIB strain	HE strain
	ng/ml		
CXCR4[WT]	13	10	12
CXCR4[D171N]	29	44	379
CXCR4[D262N]	86	>200	>1000
CXCR4[D171N,D262N]	N.A.	N.A.	>1000
CXCR4[H281A]	1.2	1.8	1.6

[a] 50% inhibitory concentration of AMD3100 for p24 antigen production, as measured by ELISA in the culture supernatant at day 5 after infection.
NA, not applicable because of lack of virus replication.

Acknowledgments

We thank Sandra Claes and Eric Fonteyn for excellent technical assistance. We are indebted to Dr. R. Förster and Dr. M. Lipp (Max Delbrück Center for Molecular Medicine, Berlin-Buch, Germany) for providing the anti-CXCR4 2B11 antibody.

References

Alkhatib G, Combadiere C, Broder CC, Feng Y, Kennedy PE, Murphy PM and Berger EA (1996) CC CKR5: a RANTES, MIP-1α, MIP-1β receptor as a fusion cofactor for macrophage-tropic HIV-1. *Science (Wash DC)* **272:**1955–1958.

Atchison RE, Gosling J, Monteclaro FS, Franci C, Digilio L, Charo IF and Goldsmith MA (1996) Multiple extracellular elements of CCR5 and HIV-1 entry: dissociation from response to chemokines. *Science (Wash DC)* **274:**1924–1926.

Berger EA, Murphy PM and Farber JM (1999) Chemokine receptors as HIV-1 coreceptors: roles in viral entry, tropism and disease. *Annu Rev Immunol* **17:**657–700.

Bjorndal A, Deng H, Jansson M, Fiore JR, Colognesi C, Karlsson A, Albert J, Scarlatti G, Littman DR and Fenyo EM (1997) Coreceptor usage of primary human immunodeficiency virus type 1 isolates varies according to biological phenotype. *J Virol* **71:**7478–7487.

Bleul CC, Farzan M, Choe H, Parolin C, Clark-Lewis I, Sodroski J and Springer TA (1996) The lymphocyte chemoattractant SDF-1 is a ligand for LESTR/fusin and blocks HIV-1 entry. *Nature (Lond)* **382:**829–832.

Brelot A, Heveker N, Montes M and Alizon M (2000) Identification of residues of CXCR4 critical for human immunodeficiency virus coreceptor and chemokine receptor activities. *J Biol Chem* **275:**23736–23744.

Bridger GJ, Skerlj RT, Thornton D, Padmanabhan S, Martellucci SA, Henson GW, Adams MJ, Yamamoto N, De Vreese K, Pauwels R, et al. (1995) Synthesis and structure-activity relationships of phenylenebis(methylene)-linked bis-tetraazamacrocycles that inhibit HIV replication. Effects of macrocyclic ring size and substituents on the aromatic linker. *J Med Chem* **38:**366–378.

Chan DC and Kim PS (1998) HIV entry and its inhibition. *Cell* **93:**681–684.

Connor RI, Sheridan KE, Ceradini D, Choe S and Landau NR (1997) Change in coreceptor use correlates with disease progression in HIV-1 infected individuals. *J Exp Med* **185:**621–628.

Datema R, Rabin L, Hincenbergs M, Moreno MB, Warren S, Linquist V, Rosenwirth B, Seifert J and McCune JM (1996) Antiviral efficacy in vivo of the anti-human immunodeficiency virus bicyclam SDZ SID 791 (JM3100), an inhibitor of infectious cell entry. *Antimicrob Agents Chemother* **40:**750–754.

Dealwis C, Fernandez EJ, Thompson DA, Simon RJ, Siani MA and Lolis E (1998) Crystal structure of chemically synthesized [N33A] stromal cell-derived factor 1α, a potent ligand for the HIV-1 "fusin"coreceptor. *Proc Natl Acad Sci USA* **95:**6941–6946.

De Clercq E, Yamamoto N, Pauwels R, Balzarini J, Witvrouw M, De Vreese K, Debyser Z, Rosenwirth B, Peichl P, Datema R, et al. (1994) Highly potent and selective inhibition of human immunodeficiency virus by the bicyclam derivative JM3100. *Antimicrob Agents Chemother* **38:**668–674.

Deng H, Liu R, Ellmeier W, Choe S, Unutmaz D, Burkhart M, Marzio PD, Marmon S, Sutton RE, Hill CM, et al. (1996) Identification of a major co-receptor for primary isolates of HIV-1. *Nature (Lond)* **381:**661–666.

De Vreese K, Reymen D, Griffin P, Steinkasserer A, Werner G, Bridger GJ, Esté JA, James W, Henson GW, Desmyter J, et al. (1996) The bicyclams, a new class of potent human immunodeficiency virus inhibitors, block viral entry after binding. *Antiviral Res* **29:**209–219.

Donzella GA, Schols D, Lin SW, Esté JA, Nagashima KA, Maddon PJ, Allaway GP, Sakmar TP, Henson G, De Clercq E, et al. (1998) AMD3100, a small molecule inhibitor of HIV-1 entry via the CXCR4 co-receptor. *Nat Med* **4:**72–77.

Endres MJ, Clapham PR, Marsh M, Ahuja M, Davis Turner J, McKnight A, Thomas JF, Stoebenau-Haggarty B, Choe S, Vance PJ, et al. (1996) CD4-independent infection by HIV-2 is mediated by Fusin/CXCR4. *Cell* **87:**745–756.

Feng Y, Broder CC, Kennedy PE and Berger EA (1996) HIV-1 entry cofactor: functional cDNA cloning of a seven-transmembrane, G protein-coupled receptor. *Science (Wash DC)* **272:**872–877.

Förster R, Kremmer E, Schubel A, Breitfeld D, Kleinschmidt A, Nerl C, Bernhardt G and Lipp M (1998) Intracellular and surface expression of the HIV-1 coreceptor CXCR4/Fusin on various leukocyte subsets: rapid internalization and recycling upon activation. *J Immunol* **160:**1522–1531.

Gerlach LO, Skerlj RT, Bridger GJ and Schwartz TW (2001) Molecular interactions of cyclam and bicyclam non-peptide antagonists with the CXCR4 chemokine receptor. *J Biol Chem* **276:**14153–14160.

Hendrix CW, Flexner C, MacFarland RT, Giandomenico C, Fuchs EJ, Redpath E, Bridger G and Henson GW (2000) Pharmacokinetics and safety of AMD-3100, a novel antagonist of the CXCR-4 chemokine receptor, in human volunteers. *Antimicrob Agents Chemother* **44:**1667–1673.

Ho SN, Hunt HD, Horton RM, Pullen JK and Pease LR (1989) Site-directed mutagenesis by overlap extension using the polymerase chain reaction. *Gene* **77:**51–59.

Iyengar S, Hildreth JE and Schwartz DH (1998) Actin-dependent receptor colocalization required for human immunodeficiency virus entry into host cells. *J Virol* **72:**5251–5255.

Johansen TE, Scholler MS, Tolstoy S and Schwarz TW (1990) Biosynthesis of peptide precursors and protease inhibitors using new constitutive and inducible eukaryotic expression vectors. *FEBS Lett* **267:**289–294.

Kajumo F, Thompson DA, Guo Y and Dragic T (2000) Entry of R5X4 and X4 human immunodeficiency virus type 1 strains is mediated by negatively charged and tyrosine residues in the amino-terminal domain and the second extracellular loop of CXCR4. *Virology* **271:**240–247.

Labrosse B, Brelot A, Heveker N, Sol N, Schols D, De Clercq E and Alizon M (1998) Determinants for sensitivity of human immunodeficiency virus coreceptor CXCR4 to the bicyclam AMD3100. *J Virol* **72:**6381–6388.

Lapham CK, Zaitseva MB, Lee S, Romanstseva T and Golding H (1999) Fusion of monocytes and macrophages with HIV-1 correlates with biochemical properties of CXCR4 and CCR5. *Nat Med* **5:**303–308.

Murdoch C and Finn A (2000) Chemokine receptors and their role in inflammation and infectious diseases. *Blood* **95:**3032–3043.

Oberlin E, Amara A, Bachelerie F, Bessia C, Virelizier JL, Arenzana-Seisdedos F, Schwartz O, Heard JM, Clark-Lewis I, et al. (1996) The CXC chemokine SDF-1 is the ligand for LESTR/fusin and prevents infection by T-cell-line-adapted HIV-1. *Nature (Lond)* **382:**833–835.

Pauwels R, Andries K, Desmyter J, Schols D, Kukla MJ, Breslin HJ, Raeymaeckers A, Van Gelder J, Woestenborghs R, Heykants J, et al. (1990) Potent and selective inhibition of HIV-1 replication *in vitro* by a novel series of TIBO derivatives. *Nature (Lond)* **343:**470–474.

Ratner L, Haseltine W, Patarca R, Livak KJ, Starcich B, Josephs SF, Doran ER, Rafalski JA, Whitehorn EA, Baumeister K, et al. (1985) Complete nucleotide sequence of the AIDS virus, HTLV-III. *Nature (Lond)* **313:**277–284.

Schols D, Esté JA, Henson G and De Clercq E (1997a) Bicyclams, a class of potent anti-HIV agents, are targeted at the HIV coreceptor Fusin/CXCR-4. *Antiviral Res* **35:**147–156.

Schols D, Struyf S, Van Damme J, Esté JA, Henson G and De Clercq E (1997b) Inhibition of T-tropic HIV strains by selective antagonization of the chemokine receptor CXCR4. *J Exp Med* **186:**1383–1388.

Send correspondence to: Sigrid Hatse, Rega Institute for Medical Research, Minderbroedersstraat 10, B-3000 Leuven, Belgium. E-mail: sigrid.hatse@rega.kuleuven.ac.be